First Frequency-time-resolved Imaging Spectroscopy Observations of Solar Radio Spikes

d.clarkson.2@research.gla.ac.uk

Published in Clarkson+2021, ApJL, 917, L32

Daniel L. **Clarkson**[1], Eduard P. **Kontar**[1], Mykola **Gordovskyy**[2], Nicolina **Chrysaphi**[3,1], Nicole **Vilmer**[3,4]

[1]University of Glasgow, [2]University of Manchester, [3]LESIA, Observatoire de Paris, [4]Station de Radioastronomie de Nançay, Observatoire de Paris

1. Introduction

Solar radio spikes are short duration, narrowband radio bursts that are a signature of the acceleration of non-thermal electrons in solar flares. They are observed over a wide range of frequencies (tens of MHz to GHz) and their high brightness temperatures indicate coherent mechanisms: plasma emission, or electron cyclotron maser (ECM) emission. Previous spike imaging observations have been conducted at high frequencies. In this study, we show for the first time, the frequency and time resolved evolution of individual radio spikes using the imaging capabilities of the LOw Frequency ARray (LOFAR) and the determination of their morphological characteristics between 30-70 MHz.

2. Why Study Spikes?

- Their origin is not fully understood.
- Their short duration & narrow frequency range are indicative of processes that occur on millisecond timescales.
- They provide an avenue to study the fastest processes in the solar corona.
- Their short durations represent an upper limit for the energy release time.

3. LOFAR

- Radio interferometer with tied-array digital beamforming capable of observing between 10-250 MHz.
- We use the Low Band Antenna between 30-70 MHz with a temporal and spectral resolution of 10 ms and 12.2 kHz.
- Provides the capability to resolve radio burst fine structure over tens of millisecond scales, with tracking of the centroid motion & burst sizes over both time and frequency.

The author would like to thank DSTL for the funding received for this project through the UK France PhD Scheme.

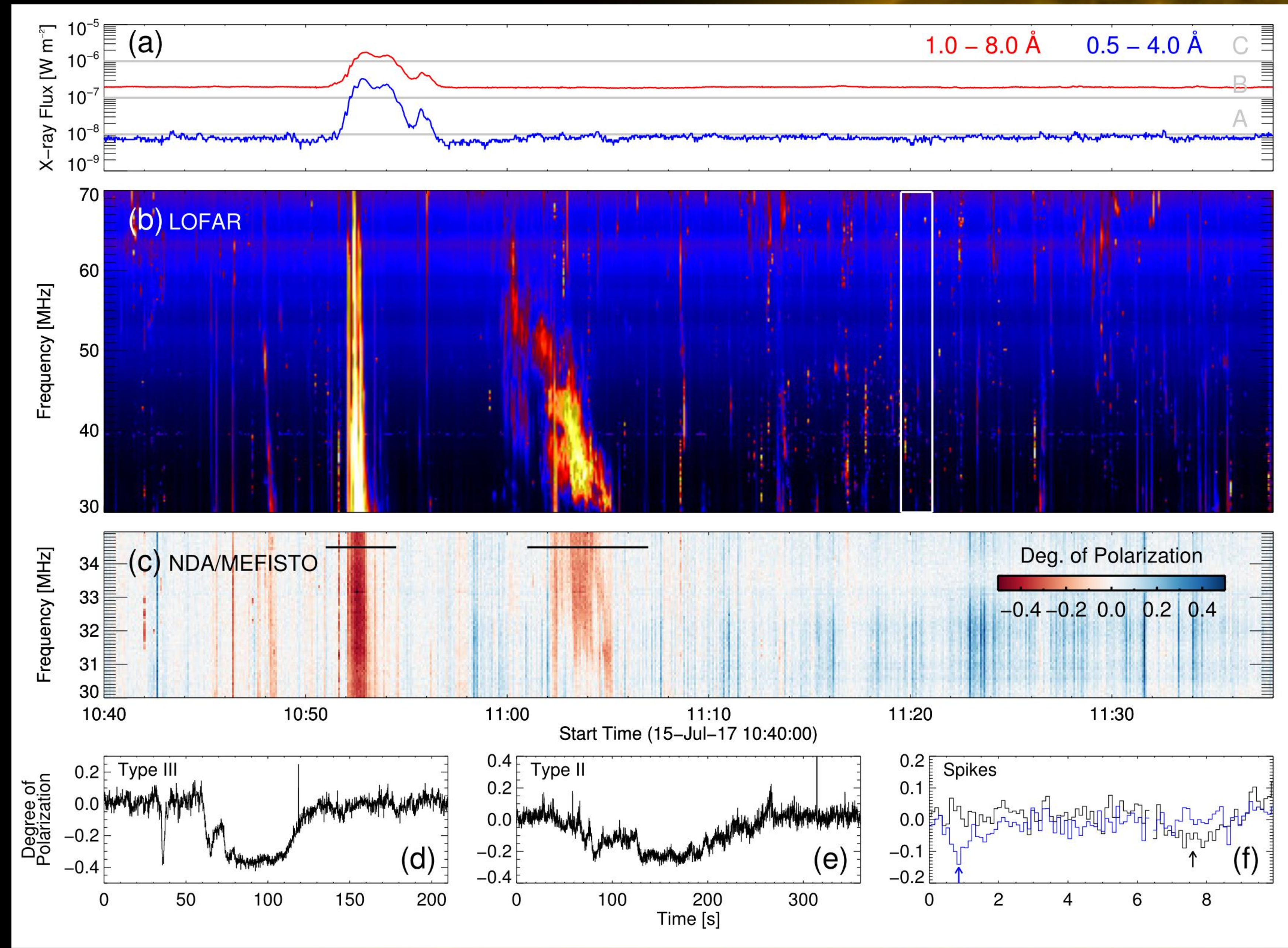

Figure 1 (above): X-ray and radio emissions between 10:40 and 11:40 UT. **(a)** X-ray lightcurves from the GOES spacecraft **(b)** Dynamic spectrum of the LOFAR observation. The white box represents the region shown in Figure 2a. **(c)** NDA/MEFISTO polarization. **(d-f)** Type III, Type II and individual spike polarizations.

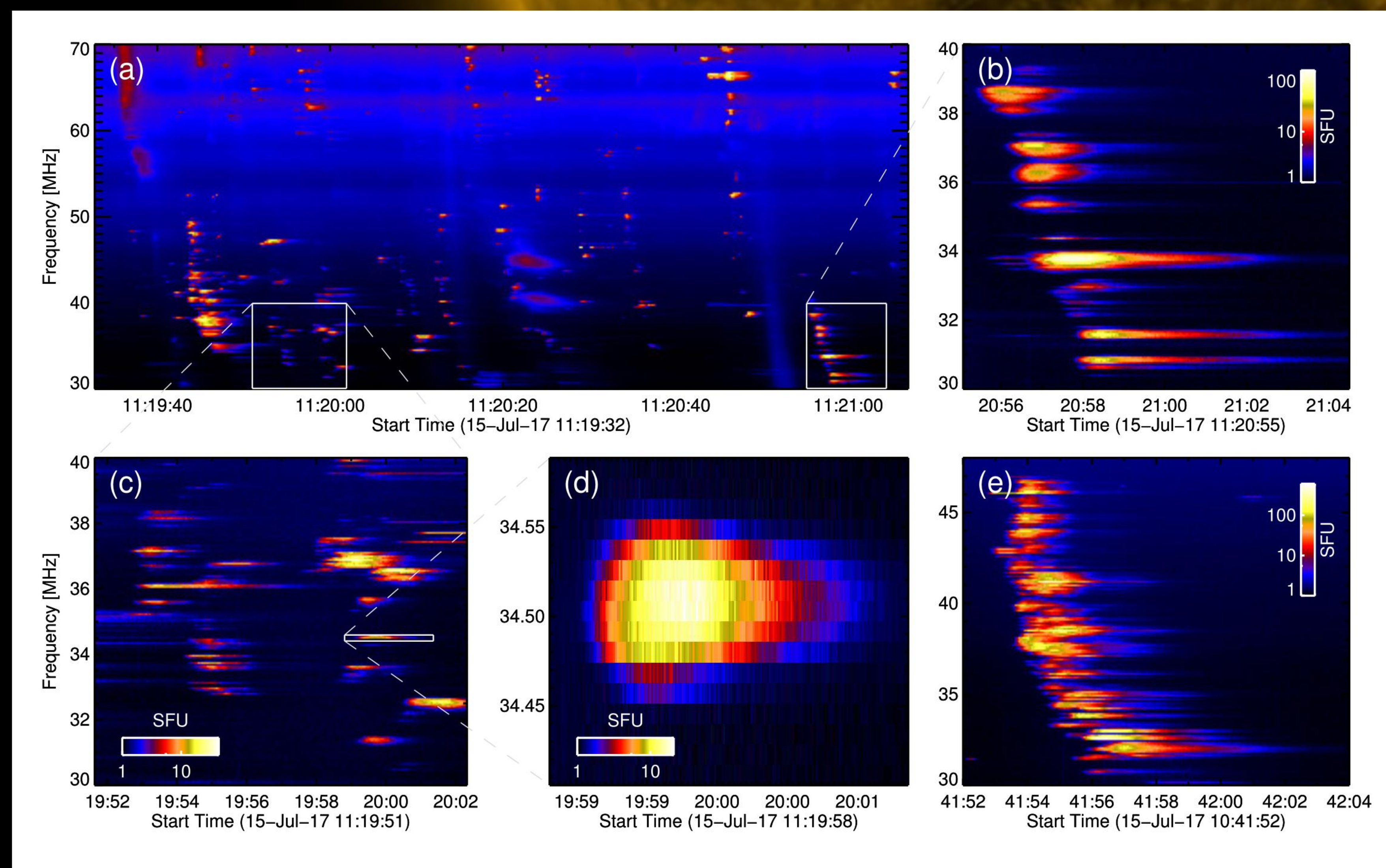

Figure 2 (above): Zoomed in dynamic spectra of spike and Type IIIb features within Figure 1. **(a)** The region bounded by the white box in Figure 1b. **(b)** Type IIIb burst near 11:21 UT (post-CME). **(c)** Spike cluster (post-CME). **(d)** An individual spike. **(e)** Type IIIb burst observed near 10:42 UT (pre-CME).

4. LOFAR Observations

1 hour overview dynamic spectra are shown in Figure 1.

- The brightest features are a series of Type III bursts, a Type II burst originating from a CME (Chrysaphi+2020), and numerous Type IIIb bursts.
- The main spike cluster occurs after the Type II, with a smaller number of spikes occurring pre-CME.
- The spike and Type III/IIIb/II bursts show left-hand circular polarization.

Figure 2 shows zoomed-in dynamic spectra of the spikes and Type IIIb striae. A spike cluster can be seen in panel (c) where spikes are randomly distributed. A single well isolated spike is shown in panel (d). Panels (b,e) show the two Type IIIb bursts where individual striae properties are compared to spikes (Figure 3).

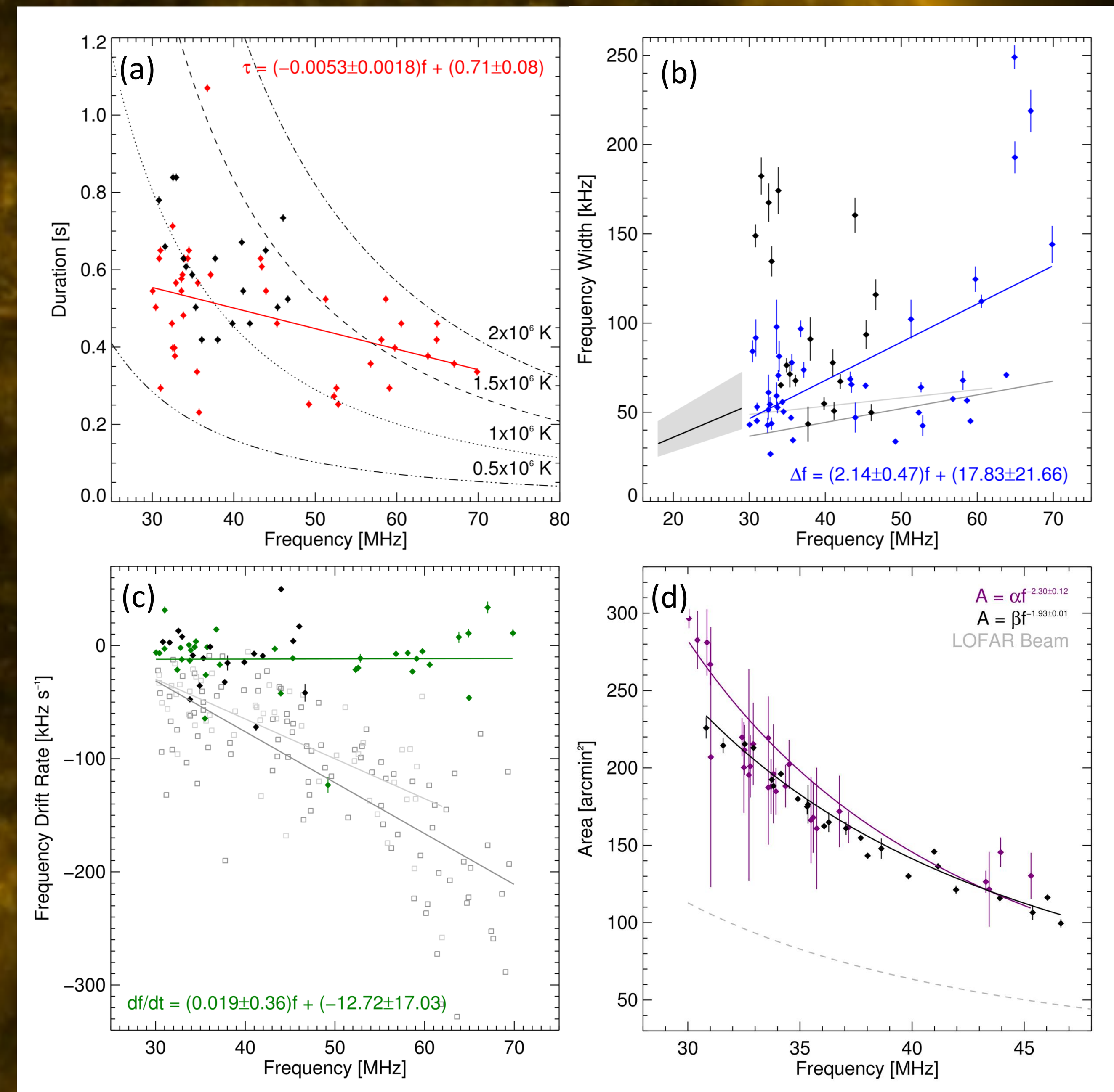

Figure 3 (above): Spike (coloured) & striae (black) characteristics **(a)** Duration. **(b)** Frequency width. The black line shows the average fit to spike widths from Melnik+(2014). Grey thin lines show fits to striae widths from Sharykin+(2018). **(c)** Frequency drift. Grey squares and lines show striae drifts from Sharykin+(2018). **(d)** Area.

5. Spike Characteristics

Figure 3 shows various spike characteristics against frequency, with spikes shown in coloured points, and striae in black.

- In all plots, spikes and striae characteristics are very similar.
- Spikes durations are comparable to the plasma collision time, indicating that damping within the plasma could be one of the factors that determines the observed duration.
- Spectral widths tend to increase with frequency, consistent with spike measurements at lower and higher frequencies.
- Drift rates infer exciter velocities between 10-50 km s^{-1}.
- Areas decrease with increasing frequency.

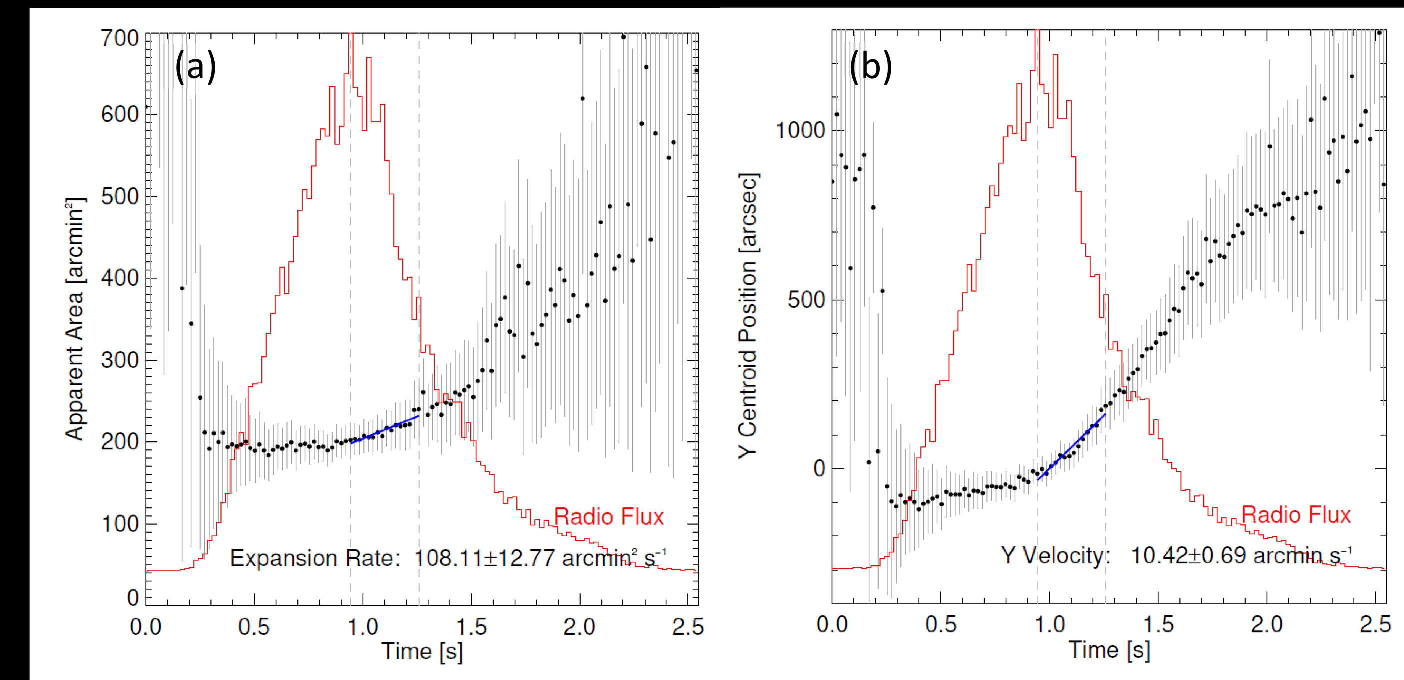

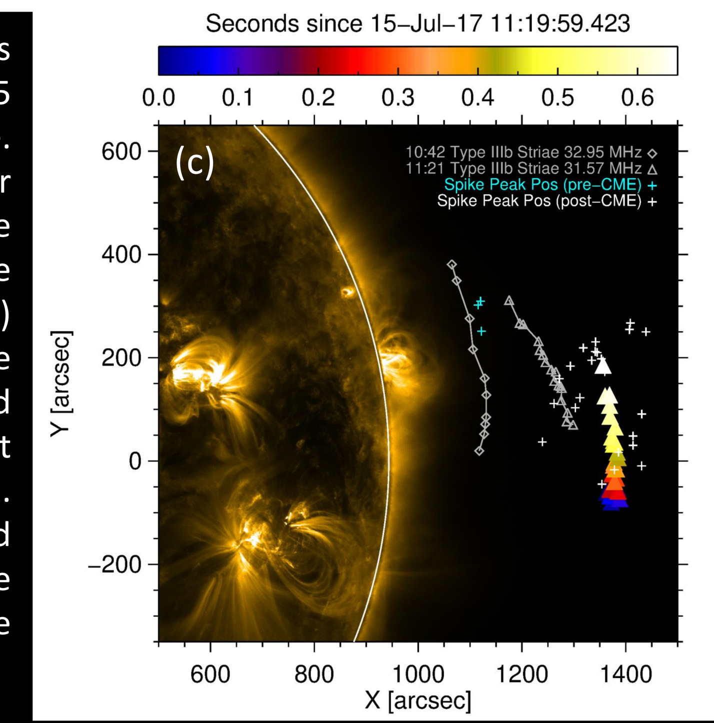

Figure 4 (above/right): Temporal properties of the spike shown in Figure 2d at 34.5 MHz. **(a)** Observed FWHM area over time. **(b)** Spike vertical centroid motion over time. The red curves represent the normalised spike lightcurve. **(c)** Spike centroid motion (coloured triangles) overlaid on an SDO/AIA 171 Å image. The blue plus symbols show the peak centroid position of other spikes pre-CME, whilst white plus symbols show those post-CME. The grey lines with diamond (pre-CME) and triangle (post-CME) markers represent the centroid motion of two individual striae from Figure 2(b,e).

6. Scattering Effects & Superluminal Motion

- One of the intriguing observations is that the spike (and striae) motion is not radial, but parallel to the solar limb (Figure 4a).
- Apparent spike centroid motions show **superluminal** speeds (Figure 4b) caused by scattering due to **anisotropic density turbulence**.
- Scattering induces a shift of the emission in the direction of the guiding magnetic field, suggesting closed loop magnetic field structures with strong levels of anisotropy.
- Larger apparent source velocities & greater observed displacement occurs at larger heliocentric angles (Kontar+2019, Kuznetsov+2020).

7. Emission Mechanism

- Co-spatial origin of spikes & striae, their morphological similarity & matching polarization suggests a common exciter.
- The coronal height suggests ECM emission is infeasible.
- We suggest the plasma emission mechanism as the spike source, similar to Type IIIb bursts, from weaker/slower electron beams.

8. Conclusion

- Low-frequency radio spikes are strongly affected by scattering due to the radiation escaping through anisotropic density turbulence, with scattering preferentially along the guiding magnetic field.
- The scattering dominance acts to extend the spike time profile, implying that the energy release time is shorter than often assumed.
- Density turbulence anisotropy could be higher along closed field lines.
- Spikes & striae show similar characteristics, suggesting the spikes are generated by the plasma emission mechanism.

Chrysaphi et al. (2020), *ApJ*, 893, 115
Kontar et al. (2019), *ApJ*, 884, 112
Kuznetsov et al. (2020), *ApJ*, 898, 94
Melnik et al. (2014), *SoPh*, 289, 1701
Sharykin et al. (2018), *SoPh*, 219, 115